

Chapter 4

Enrichment Factors of Perfluoroalkyl Oxoanions at the Air/Water interface*

* This chapter is reproduced with permission from E. Psillakis, J. Cheng, M. R. Hoffmann, and A. J. Colussi, *Journal of Physical Chemistry A*, **2009**, 113, 8826. Copyright © 2009, American Chemical Society

4. 1 Abstract

The refractory, water-bound perfluoro-*n*-alkyl carboxylate $F(CF_2)_nCO_2^-$ and sulfonate $F(CF_2)_nSO_3^-$ surfactant anions reach remote locations by mechanisms that are not well understood. Here we report experiments in which the relative concentrations of these anions on the surface of microdroplets produced by nebulizing their aqueous solutions are measured via electrospray ionization mass spectrometry. Enrichment factors f (relative to Br^- : $f(Br^-) \equiv 1$) increase with n , asymptotically reaching $f[F(CF_2)_nSO_3^-] \sim 2 f[F(CF_2)_nCO_2^-] \sim 200 f(Br^-)$ values above $n \sim 8$. The larger f values for $F(CF_2)_nSO_3^-$ over their $F(CF_2)_nCO_2^-$ congeners are consistent with a closer approach of the bulkier, less-hydrated $-SO_3^-$ headgroup to the air/water interface. A hyperbolic, rather than the predicted linear $\log f[F(CF_2)_nCO_2^-]$ vs. n dependence suggests the onset of conformational restrictions to interfacial enrichment above $n \sim 4$. Marine aerosols produced from contaminated ocean surface waters are therefore expected to be highly enriched in $F(CF_2)_nCO_2^-/F(CF_2)_nSO_3^-$ species.

4.2 Introduction

The exceptionally persistent perfluoroalkyl (*F*-alkyl) sulfonates, $F(CF_2)_nSO_3^-$, and *F*-alkyl carboxylates, $F(CF_2)_nCO_2^-$, surfactants have spread and bioaccumulated globally since their inception ~50 years ago.¹⁻⁴ Because their strong conjugated *F*-alkyl acids ($pK_a < 1$)⁵ are fully dissociated in water (particularly in seawater pH ~ 8.1) oceans are expected to be the main reservoir, and ocean currents the ultimate conduits for these water-bound anions.⁶⁻¹⁰ *F*-alkyl anions, however, reach water bodies and continental sites far removed from both sources and oceans.⁹ The short (within oceanic transport time frames) bioaccumulation times and decay half-life of $F(CF_2)_8SO_3^-$ in Canadian Arctic seals after its phase-out¹¹⁻¹² suggest an atmospheric mechanism of dispersal.^{8,10,13}

F-alkyl anions can be indirectly transported by gaseous alcohol (PFOH) and sulfonamide (PFSN) precursors.¹⁴ However, *F*-alkyl surfactant anions can also be aerosolized.^{8,10,15-16} There is conclusive evidence that aerosols produced from the ocean's uppermost microlayer are highly enriched in ionic and non-ionic amphiphiles, carrying them far afield over continental masses.¹⁶⁻²⁹ Fine aerosol particles may be transported over 10^2 – 10^3 km without settling.³⁰ The recently reported spatial and depth concentration profiles of several *F*-alkyl anions in the world's oceans, particularly in the Labrador Sea and the Middle Atlantic Ocean,⁷ together with regional atmospheric and oceanic circulation patterns,³¹⁻³⁹ could provide key data to test whether the aerosolization of marine *F*-alkyl anions is a key stage in their global dispersal.^{8,13,40-41}

Partition coefficients of *F*-alkyl acids between *n*-octanol and water have been estimated empirically and theoretically without experimental validation.⁴² Until very recently,⁴³ no information was available on the partitioning of their hydrophobic

anions between water and organic solvents, although it had been reported that perfluorooctyl oxoanions could be extracted from biological matrices into methyl *tert*-butyl ether as tetrabutylammonium salts for subsequent mass spectrometric detection.⁴⁴⁻⁴⁵ Selective partition of the perfluorooctyl species versus chloride from water into lipophilic polymer membranes or fluoruous solvents had been previously demonstrated by potentiometry.⁴⁶

We have recently investigated the fractionation of globular anions at the air/water interface using a novel approach in which relative interfacial anion concentrations in microdroplets produced by pneumatic nebulization of multicomponent solutions are simultaneously measured by online thermospray ionization mass spectrometry.^{17,47-48} Here we report the dynamic enrichment factors of various *F*-alkyl anions at the air/water interface, and analyze their physicochemical and environmental implications.

4.3 Experimental Section

Sodium acetate (EM Science 99%), CF₃COOH (Aldrich 99%), CH₃SO₃Na and CF₃SO₃Na (Aldrich 98%), NaCl, NaBr, NaI, NaNO₃, NaClO₄ and NaSCN (> 98%, Aldrich), sodium dodecylsulfate (SDS, Baker), 1-octanol (Aldrich), potassium *F*-butane-1-sulfonate (4-PFSK 98%, Aldrich), potassium *F*-hexane-1-sulfonate (6-PFSO₃K 98%, Fluka), potassium *F*-octane-1-sulfonate (8-PFSO₃K 98%, Fluka), *F*-butyric acid (3-PFCO₂H, 98%, Aldrich), *F*-pentanoic acid (4-PFCO₂H, 97%, Aldrich), *F*-hexanoic acid (5-PFCO₂H, 97%, Fluka), *F*-heptanoic acid (6-PFCO₂H, 99%, Aldrich), *F*-octanoic acid (7-PFCO₂H, 97%, Aldrich), and *F*-nonanoic acid (8-PFCO₂H, 97%, Aldrich), were used as received. Individual stock solutions (1 mM) were prepared with Milli-Q water (resistivity 18.2 MΩ cm) in borosilicate bottles.

Negative ion mass spectra of multicomponent aqueous solutions (1 μM in each surfactant unless otherwise indicated) were obtained via direct infusion into a

commercial thermospray ionization mass spectrometer (ESI-MS, HP-1100 MSD) operated under the following conditions: drying gas flow, 10 L min⁻¹; drying gas temperature, 340 °C; nebulizer pressure, 28 psi; collector capillary voltage, 3.5 kV; fragmentor voltage, 80 V. Solutions were pumped (50 μL/min) into the spraying chamber of the mass spectrometer through a *grounded* stainless steel needle inserted in a coaxial sheath issuing nebulizer N₂ gas. The high velocity nebulizer gas breaks up the liquid jet into a conical mist of microdroplets carrying net charges of either sign.⁴⁹⁻⁵³ Pneumatic nebulization generates weakly negatively charged microdroplets.⁴⁹ Fast solvent evaporation leads to droplet shrinkage and concomitant surface charge crowding.⁵⁴ Droplets become mechanically unstable when electrostatic repulsion among charges overcomes liquid cohesion, and spontaneously shed their interfacial films into even smaller droplets. A series of these events ultimately leads to nanodroplets from which unsolvated ions are electrostatically ejected into the gas phase.⁵⁵⁻⁵⁹ Gas-phase ions are then deflected into the mass spectrometer by applying a suitable electric bias to its inlet port orthogonal to the injector. It has been shown that surfactant species tend to accumulate in the periphery of the conical mist,⁶⁰ i.e., precisely in the finer microdroplets sampled by the orthogonal port.⁴⁷ This technique therefore probes the composition of nanodroplets created from the interfacial layers of the microdroplets produced by pneumatic nebulization of test solutions.

Mass spectra were acquired in single ion mode preset at $m/z = [149 + (n - 1) 50]$ for $F(CF_2)_nSO_3^-$, at $[69 + (n - 1) 50]$ and $[113 + (n - 1) 50]$ for $F(CF_2)_nCO_2^-$, 58 and 60 (^{32,34}SCN⁻), 62 (NO₃⁻), 79 and 81 (^{79,81}Br⁻), 99 and 101 (^{35,37}ClO₄⁻), 127 (I⁻), and 265 (SDS). MS signal intensities for the various *F*-alkyl anions were found to increase linearly with the concentration of their solutions in the range 0.1 to 5 μM, relative to the $m/z = 265$ signal of 0.2 μM SDS used as a reference (Figure 4.1). Repeatability

and reproducibility of the derived enrichment factors f (see below), expressed as % RSD, were better than 2.5% and 4%, respectively. Reported data are the average of at least duplicate runs.

4.4 Results and Discussion

Under present instrumental settings, $F(CF_2)_nSO_3^-$ are detected as molecular monoanions (M) at $[149 + (n - 1) 50]$ Da, whereas $F(CF_2)_nCO_2^-$ decarboxylate significantly and appear both at $[113 + (n - 1) 50]$ Da (M) and $[69 + (n - 1) 50]$ Da (M - CO_2). The relative enrichment factor of anion i , $f(i)$, is defined herein as the sum of the mass spectral signal intensities of the j ions originating from this species: $\sum S_{i,j}$, divided by those for $^{79,81}Br^-$, the least-enriched anion of the set, measured (or extrapolated) at the same bulk molar concentration:

$$f(i) = \frac{\sum_j S_{i,j}}{S_{79} + S_{81}} \quad (4.1)$$

The $f[F(CF_2)_nSO_3^-]$ s and $f[F(CF_2)_nCO_2^-]$ s calculated using equation (4.1) and the data from Figure 4.2 and Table 4.1 are shown in Figure 4.3. $f(i) > f_{Br^-} \equiv 1$ signifies that the i -anion is enriched relative to Br^- at the air/water interfacial layers monitored in these experiments. It should be emphasized that f s are lower bounds to absolute enrichment factors because Br^- itself is slightly enriched relative to Cl^- , which has been shown to be nearly neutral toward interfacial enrichment.⁶¹⁻⁶² Since $f(i)$ were determined at, or scaled to 1 μ M in all cases, they are proportional to the partition coefficient between bulk water (B) and its aerial interface (S):⁶³

$$f(i) \propto K_i = \frac{x_i^S}{x_i^B} \quad (4.2)$$

$$\log f(i) \propto -\frac{\Delta G_{B \rightarrow S}^o(i)}{4.6kT} \quad (4.3)$$

where x_i^P represents the molar fraction of i in phase P , and $\Delta G_{B \rightarrow S}^\circ$ the molar free energy released upon transferring i from the bulk to the air/water interface.

Figure 4.3 shows that f_s for carboxylates are most sensitive to alkyl chain length between $n = 1$ and 3 and appear to plateau beyond $n = 9$. It is apparent that both $F(\text{CF}_2)_n\text{SO}_3^-$ and $F(\text{CF}_2)_n\text{CO}_2^-$ are highly enriched at the interface, with $f[\text{F}(\text{CF}_2)_n\text{SO}_3^-] \sim 2.3 f[\text{F}(\text{CF}_2)_n\text{CO}_2^-] \sim 190 f(\text{Br}^-)$ as $n \rightarrow \infty$ (Figure 4.3). Figure 4.4 shows that the addition of 100 μM electrolyte tends to depress f_s for the shorter, least-enriched homologues and enhance those for higher members of both carboxylate and sulfonate classes. A similar trend is observed upon saturation with 1-octanol. These phenomena are consistent with the competition of various solutes for the air/water interface. Simple anions at 100 μM will crowd the interface in competition with surfactant anions at 1 μM . Short F -alkyl chain surfactant anions will be rejected, whereas the longer homologues will be expelled from the interface by electrostatic forces.

We have previously shown that f_s for globular anions at air/liquid interfaces increase exponentially with ionic radius R .⁴⁸ Hydrated ions have a smaller dielectric constant than water and will be expelled to the interface by many-body electrodynamic dispersive interactions that scale with R .^{48,64-65} Since the sulfonate headgroup is larger than the carboxylate, $f[\text{F}(\text{CF}_2)_n\text{SO}_3^-]$ s are predictably larger than $f[\text{F}(\text{CF}_2)_n\text{CO}_2^-]$ s (Figure 4.3, Table 4.1). This result is consistent with previous observations that the alkyl sulfonates with a larger ionic radius is more lipophilic than the corresponding carboxylate at water/1,2-dichloroethane or nitrobenzene interfaces.⁴⁶ Perfluorination enhances anion partitioning to the aerial interface, viz.: $f(\text{CF}_3\text{SO}_3^-)/f(\text{CH}_3\text{SO}_3^-) = 2.7$, $f(\text{CF}_3\text{COO}^-)/f(\text{CH}_3\text{COO}^-) = 3.0$ (see Table 4.1).⁶⁶

From equations (4.2)-(4.4), enrichment factors of F -alkyl surfactants f should increase exponentially with n .⁶³

$$\Delta G_{B \rightarrow S}^o[\text{F}(\text{CF}_2)_n \text{CO}_2^-] = \Delta G_P^o + n \Delta G_{B \rightarrow S}^o(\text{CF}_2) \quad (4.4)$$

if the $\Delta G_{B \rightarrow S}^o(\text{CF}_2) = \Delta G_{B \rightarrow \text{AIR}}^o(\text{CF}_2) + \Delta G_{\text{AIR} \rightarrow S}^o(\text{CF}_2) = -2.74 - 2.32 = -5.06 \text{ kJ mol}^{-1}$ ⁶⁷⁻⁶⁸ group contribution to the molar free energy of $B \rightarrow S$ transfer were independent of n . ΔG_P^o is the contribution of the headgroup plus the difference between the CF_3 - and CF_2 -group contributions. Note that both $\Delta G_{B \rightarrow S}^o(\text{CF}_2)$ and $\Delta G_{\text{AIR} \rightarrow S}^o(\text{CF}_2)$ are negative, meaning that the location of lowest free energy for CF_2 groups is the interface. Since linear $\log f$ vs. n dependences have been verified for most surfactant classes,⁶³ enrichment factors for F -alkyl surfactant homologues were expected to increase as $f[\text{F}(\text{CF}_2)_n \text{CO}_2^-]/f[\text{F}(\text{CF}_2)_{n-1} \text{CO}_2^-] = \exp[-\Delta G_{B \rightarrow S}^o(\text{CF}_2)/2kT] = 2.7$ at 300 K. Figures 4.2 and 4.3, and Table 4.1 show that this is not the case. Neither $\log f$ increases linearly with n , nor $f[\text{F}(\text{CF}_2)_8 \text{CO}_2^-]/f[\text{F}(\text{CF}_3) \text{CO}_2^-]$ exceeds ~ 28 (vs. $2.7^7 \sim 1244$). Instead, we find that $\log f[\text{F}(\text{CF}_2)_n \text{CO}_2^-]$ increases as predicted up to $n \sim 3$, and considerably less so afterward (Figure 4.3). The experimental $f[\text{F}(\text{CF}_2)_n \text{CO}_2^-]/f[\text{F}(\text{CF}_2)_{n-1} \text{CO}_2^-] \sim 1.16$ (vs. 2.7) in the range $3 \leq n \leq 8$ effectively corresponds to $\Delta G_{B \rightarrow S}^o(\text{CF}_2) = -0.74 \text{ kJ mol}^{-1}$ (vs. $-5.06 \text{ kJ mol}^{-1}$). Since $f(\text{PF}_6^-)$, which has a similar value to $f[\text{F}(\text{CF}_2)_8 \text{SO}_3^-]$, adhered to the linear $\log f$ vs. R correlation followed by smaller anions,⁴⁷⁻⁴⁸ we infer that non-linearity is not due to dynamic range limitations and less-than-linear instrumental response but likely reflects molecular properties of the F -alkyl chain. It is also possible, given the dynamic nature of our experiments, that the microdroplets surfaces we probe here might not be fully equilibrated with these highly surface-active species. However, since a similar limitation is expected to apply to F -alkyl oxoanion surfactant partitioning during bubble bursting events,^{34,35} we believe that our results are particularly relevant to surfactant enrichment in aerosols of marine origin.

In this context, the rather sharp inflection in the $\log f[\text{F}(\text{CF}_2)_n\text{CO}_2^-]$ vs. n plot (Figure 4.3) amounts to a 4.32 kJ mol^{-1} increase of the net $\Delta G_{B \rightarrow S}^0(\text{CF}_2)$ contribution beyond $n \sim 3$. Since $\Delta G_{AIR \rightarrow S}^0(\text{CF}_2) = -2.32 \text{ kJ mol}^{-1}$ ⁶⁷ thermodynamics dictates that *F*-alkyl chains should tend to lie flat on the water surface.⁶⁹ Scheme 4.1 shows that the (most stable in an isotropic and homogeneous medium) *anti* $\text{F}(\text{CF}_2)_3\text{CO}_2^-$ rotamer at the air/water interface is unable to maximize the attractive dispersive interactions of *F*-alkyl chains with the water surface, a restriction that is relaxed by a $\pm 90^\circ$ torsion about the $\text{C}_2\text{-C}_3$ bond. It is apparent that only the *syn* rotamer can keep the headgroup immersed and the *F*-alkyl chain bent over the water surface.

A recent report suggests that the higher lipophilicity of *F*-alkyl oxoanions relative to their alkyl counterparts is actually due to the electron-withdrawing effect of the *F*-alkyl chain on the headgroup,⁴³ because the insertion of a $(\text{CH}_2)_2$ spacer between a perfluorohexyl chain and the $-\text{CO}_2\text{H}$ group increases the pK_a of the latter by 2.32 units, and reduces about 400 times the lipophilicity of the corresponding nonanoate. We wish to point out that both outcomes could not be physically correlated were interfacial partitioning actually involved. Distance effects on electron withdrawal from oxoanion headgroups by CF_2 moieties would be probably responsible for changes in acidity, whereas the large concomitant reduction of lipophilicity could be due to the loss of the dominant $\text{C}(2)\text{F}_2$ and $\text{C}(3)\text{F}_2$ hydrophobic contributions to interfacial partitioning.

Positive fractionation to the air/water interface underlies surfactant enrichment in the microdroplets probed in our experiments, as well as in the aerosol droplets produced via bubble bursting over the oceans.²⁴ Because microdroplets are electrically charged, in our experiments as well as in the atmospheric aerosol,^{17,70} solvent evaporation may induce further fragmentation into progeny droplets. A

cascade of these events is equivalent to a distillation process in which solute enrichment is multiplicatively amplified at each stage, i.e., the net fractionation after m stages will be given by $f_m = (f_1)^m$. The implication is that the most enriched marine aerosol droplets will be the finest, i.e., those whose settling velocity is lowest,⁷¹ have the longest atmospheric lifetimes and can, therefore, be transported farther and at higher altitudes.^{23,72} The bioaccumulation rates of *F*-alkyl oxoanions in water- or air-breathing animals, including humans, depends on their partitioning from lipids to water or air interfaces, respectively.⁷³ Our results, in conjunction with Jing et. al., data,⁴³ show that aqueous perfluorosurfactant oxoanions may have similar affinities for 1-octanol and air interfaces. Further work is underway.

4.5 Acknowledgments

This project was financially supported by the National Science Foundation (ATM-0534990). E. P. is grateful to the Fullbright Foundation for financial support.

4.6 References

- (1) Houde, M.; Martin, J. W.; Letcher, R. J.; Solomon, K. R.; Muir, D. C. G. *Environ. Sci. Technol.* **2006**, *40*, 3463.
- (2) Shoeib, M.; Harner, T.; Vlahos, P. *Environ. Sci. Technol.* **2006**, *40*, 7577.
- (3) Giesy, J. P.; Kannan, K. *Environ. Sci. Technol.* **2001**, *35*, 1339.
- (4) Giesy, J. P.; Kannan, K. *Environ. Sci. Technol.* **2001**, *35*, 1339.
- (5) Goss, K. U. *Environ. Sci. Technol.* **2008**, *42*, 456.
- (6) Wania, F. *Environ. Sci. Technol.* **2007**, *41*, 4529.
- (7) Yamashita, N.; Taniyasu, S.; Petrick, G.; Wei, S.; Gamo, T.; Lam, P. K. S.; Kannan, K. *Chemosphere* **2008**, *70*, 1247.

- (8) Young, C. J.; Furdui, V. I.; Franklin, J.; Koerner, R. M.; Muir, D. C. G.; Mabury, S. A. *Environ. Sci. Technol.* **2007**, *41*, 3455.
- (9) Simcik, M. F. *J. Environ. Monit.* **2005**, *7*, 759.
- (10) Armitage, J.; Cousins, I. T.; Buck, R. C.; Prevedouros, K.; Russell, M. H.; MacLeod, M.; Korzeniowski, S. H. *Environ. Sci. Technol.* **2006**, *40*, 6969.
- (11) Olsen, G. W.; Mair, D. C.; Church, T. R.; Ellefson, M. E.; Reagen, W. K.; Boyd, T. M.; Herron, R. M.; Medhdizadehkashi, Z.; Nobilett, J. B.; Rios, J. A.; Butenhoff, J. L.; Zobel, L. R. *Environ. Sci. Technol.* **2008**, *42*, 4989.
- (12) Renner, R. *Environ. Sci. Technol.* **2008**, *42*, 4618.
- (13) Powley, C. R.; George, S. W.; Russell, M. H.; Hoke, R. A.; Buck, R. C. *Chemosphere* **2008**, *70*, 664.
- (14) Schenker, U.; Scheringer, M.; Macleod, M.; Martin, J. W.; Cousins, I. T.; Hungerbuhlert, K. *Environ. Sci. Technol.* **2008**, *42*, 3710.
- (15) Prevedouros, K.; Cousins, I. T.; Buck, R. C.; Korzeniowski, S. H. *Environ. Sci. Technol.* **2006**, *40*, 32.
- (16) McMurdo, C. J.; Ellis, D. A.; Webster, E.; Butler, J.; Christensen, R. D.; Reid, L. K. *Environ. Sci. Technol.* **2008**, *42*, 3969.
- (17) Enami, S.; Vecitis, C. D.; Cheng, J.; Hoffmann, M. R.; Colussi, A. J. *J. Phys. Chem. A* **2007**, *111*, 8749.
- (18) Liss, P. S.; Duce, R. A. *The Sea Surface and Global Change*; Cambridge University Press: Cambridge, UK, 1997.
- (19) Duce, R. A.; Hoffman, E. J. *Ann. Rev. Earth Planet. Sci.* **1976**, *4*, 187.
- (20) Rontu, N.; Vaida, V. *J. Phys. Chem. C* **2007**, *111*, 11612.
- (21) Calace, N.; Petronio, B. M.; Cini, R.; Stortini, A. M.; Pampaloni, B.; Udisti, R. *Internat. J. Environ. Anal. Chem.* **2001**, *79*, 331.

- (22) Desideri, P. G.; Lepri, L.; Udisti, R.; Checchini, L.; Del Bubba, M.; Cini, R.; Stortini, A. M. *Int. J. Environ. Anal. Chem.* **1998**, *71*, 331.
- (23) Oppo, C.; Bellandi, S.; Degli Innocenti, N.; Stortini, A. M.; Loglio, G.; Schiavuta, E.; Cini, R. *Mar. Chem.* **1999**, *63*, 235.
- (24) Blanchard, D. C. *Science* **1964**, *146*, 396.
- (25) Macintyre, F. *J. Phys. Chem.* **1968**, *72*, 589.
- (26) Macintyre, F. *Tellus* **1970**, *22*, 451.
- (27) Donaldson, D. J.; Vaida, V. *Chem. Rev.* **2006**, *106*, 1445.
- (28) Cavalli, F.; Facchini, M. C.; Decesari, S.; Mircea, M.; Emblico, L.; Fuzzi, S.; Ceburnis, D.; Yoon, Y. J.; O'Dowd, C. D.; Putaud, J. P.; Dell'Acqua, A. J. *Geophys. Res. –Atmospheres* **2004**, *109*, D24215.
- (29) Latif, M. T.; Brimblecombe, P. *Environ. Sci. Technol.* **2004**, *38*, 6501.
- (30) Seinfeld, J. H.; Pandis, S. N. *Atmospheric chemistry and physics : from air pollution to climate change*, 2nd ed.; Wiley: Hoboken, N.J. , 2006.
- (31) Hutterli, M. A.; Crueger, T.; Fischer, H.; Andersen, K. K.; Raible, C. C.; Stocker, T. F.; Siggaard-Andersen, M. L.; McConnell, J. R.; Bales, R. C.; Burkhart, J. F. *Clim. Dyn.* **2007**, *28*, 635.
- (32) Eckhardt, S.; Stohl, A.; Beirle, S.; Spichtinger, N.; James, P.; Forster, C.; Junker, C.; Wagner, T.; Platt, U.; Jennings, S. G. *Atmos. Chem. Phys.* **2003**, *3*, 1769.
- (33) Hameed, S.; Piontkovski, S. *Geophys. Res. Lett.* **2004**, *31*, L09303.
- (34) Francis, J. A.; Hunter, E.; Zou, C. Z. *J. Climate* **2005**, *18*, 2270.
- (35) Barreiro, M.; Fedorov, A.; Pacanowski, R.; Philander, S. G. *Annu. Rev. Earth Planet. Sci.* **2008**, *36*, 33.

- (36) Kieke, D.; Rhein, M.; Stramma, L.; Smethie, W. M.; Bullister, J. L.; LeBel, D. A. *Geophys. Res. Lett.* **2007**, *34*, L06605.
- (37) Dickson, B.; Yashayaev, I.; Meincke, J.; Turrell, B.; Dye, S.; Holfort, J. *Nature* **2002**, *416*, 832.
- (38) Curry, R.; Mauritzen, C. *Science* **2005**, *308*, 1772.
- (39) Peterson, B. J.; McClelland, J.; Curry, R.; Holmes, R. M.; Walsh, J. E.; Aagaard, K. *Science* **2006**, *313*, 1061.
- (40) Dietz, R.; Bossi, R.; Riget, F. F.; Sonne, C.; Born, E. W. *Environ. Sci. Technol.* **2008**, *42*, 2701.
- (41) Smithwick, M.; Norstrom, R. J.; Mabury, S. A.; Solomon, K.; Evans, T. J.; Stirling, I.; Taylor, M. K.; Muir, D. C. G. *Environ. Sci. Technol.* **2006**, *40*, 1139.
- (42) Arp, H. P. H.; Niederer, C.; Goss, K. U. *Environ. Sci. Technol.* **2006**, *40*, 7298.
- (43) Jing, P.; Rodgers, P. J.; Amemiya, S. *J. Am. Chem. Soc.* **2009**, *131*, 2290.
- (44) Hansen, K. J.; Clemen, L. A.; Ellefson, M. E.; Johnson, H. O. *Environ. Sci. Technol.* **2001**, *35*, 766.
- (45) Kannan, K.; Koistinen, J.; Beckmen, K.; Evans, T.; Gorzelany, J. F.; Hansen, K. J.; Jones, P. D.; Helle, E.; Nyman, M.; Giesy, J. P. *Environ. Sci. Technol.* **2001**, *35*, 1593.
- (46) Kihara, S.; Suzuki, M.; Sugiyama, M.; Matsui, M. *J. Electroanal. Chem.* **1988**, *249*, 109.
- (47) Cheng, J.; Vecitis, C.; Hoffmann, M. R.; Colussi, A. J. *J. Phys. Chem. B* **2006**, *110*, 25598.
- (48) Cheng, J.; Hoffmann, M. R.; Colussi, A. J. *J. Phys. Chem. B* **2008**, *112*.

- (49) Zilch, L. W.; Maze, J. T.; Smith, J. W.; Ewing, G. E.; Jarrold, M. F. *J. Phys. Chem. A* **2008**, *112*, 13352.
- (50) Dodd, E. E. *J. Appl. Phys.* **1953**, *24*, 73.
- (51) Manisali, I.; Chen, D. D. Y.; Schneider, B. B. *Trends Anal. Chem.* **2006**, *25*, 243.
- (52) Hirabayashi, A.; Sakairi, M.; Koizumi, H. *Anal. Chem* **1994**, *66*, 4557.
- (53) Van Berkel, G. J.; Pasilis, S. P.; Ovchinnikova, O. *J. Mass Spectrom.* **2008**, *43*, 1161.
- (54) Kebarle, P.; Peschke, M. *Anal. Chim. Acta* **2000**, *406*, 11.
- (55) Iribarne, J. V.; Dziedzic, P. J.; Thomson, B. A. *Int. J. Mass Spectrom. Ion Process.* **1983**, *50*, 331.
- (56) Hirabayashi, A.; Sakairi, M.; Koizumi, H. *Anal. Chem* **1995**, *67*, 2878.
- (57) Pol, J.; Kauppila, T. J.; Haapala, M.; Saarela, V.; Franssila, S.; Ketola, R. A.; Kotiaho, T.; Kostiainen, R. *Anal. Chem.* **2007**, *79*, 3519.
- (58) Nguyen, S.; Fenn, J. B. *Proc. Natl. Acad. Sci. U.S.A.* **2007**, *104*, 1111.
- (59) Yamashita, M.; Fenn, J. B. *J. Phys. Chem.* **1984**, *88*, 4671.
- (60) Tang, K.; Smith, R. D. *J. Am. Soc. Mass Spectrom.* **2001**, *12*, 343.
- (61) Pegram, L. M.; Record, M. T., Jr. *Proc. Natl. Acad. Sci. U.S.A.* **2006**, *103*, 14278.
- (62) Pegram, L. M.; Record, M. T., Jr. *J. Phys. Chem. B* **2007**, *111*, 5411.
- (63) Fainerman, V. B.; Miller, R.; Mohwald, H. *J. Phys. Chem. B* **2002**, *106*, 809.
- (64) Israelachvili, J. *Intermolecular & Surface Forces*, 2nd ed.; Academic Press: London, 1992.
- (65) Parsegian, V. A. *Van der Waals Forces*; Cambridge University Press: New York, 2006.

- (66) Shinoda, K.; Hato, M.; Hayashi, T. *J. Phys. Chem.* **1972**, *76*, 909.
- (67) Goss, K. U.; Bronner, G. *J. Phys. Chem. A* **2006**, *110*, 9518.
- (68) Goss, K. U.; Bronner, G. *J. Phys. Chem. A* **2006**, *110*, 14054.
- (69) Tyrode, E.; Johnson, C. M.; Rutland, M. W.; Day, J. P. R.; Bain, C. D. *J. Phys. Chem. C* **2007**, *111*, 316.
- (70) Reiter, R. *J. Geophys. Res.* **1994**, *99*, 10807.
- (71) Finlayson-Pitts, B. J.; Pitts, J. N. *Chemistry of the Upper and Lower Atmosphere*; Academic Press: San Diego, CA, 2000.
- (72) Cincinelli, A.; Stortini, A. M.; Checchini, L.; Martellini, T.; Del Bubba, M.; Lepri, L. *J. Environ. Monit.* **2005**, *7*, 1305.
- (73) Kelly, B. C.; Ikonomou, M. G.; Blair, J. D.; Morin, A. E.; Gobas, F. *Science* **2007**, *317*, 236.

Table 4.1. Relative anion enrichment factors f at the air/water interface

Anion	f
CH ₃ COO ⁻	0.95
^{79,81} Br ⁻	1.00
^{32,34} SCN ⁻	2.08
I ⁻	2.61
NO ₃ ⁻	2.65
CF ₃ COO ⁻	2.86
CH ₃ SO ₃ ⁻	6.65
^{35,37} ClO ₄ ⁻	13.4
F(CF ₂) ₂ COO ⁻	22.4
F(CF ₂) ₄ COO ⁻	36.1
CF ₃ SO ₃ ⁻	37.9
H(CH ₂) ₁₂ OSO ₃ ⁻	42.8
F(CF ₂) ₅ COO ⁻	45.0
F(CF ₂) ₃ COO ⁻	46.3
F(CF ₂) ₆ COO ⁻	55.9
F(CF ₂) ₇ COO ⁻	77.9
F(CF ₂) ₈ COO ⁻	79.6
F(CF ₂) ₄ SO ₃ ⁻	133.8
F(CF ₂) ₆ SO ₃ ⁻	175.2
F(CF ₂) ₈ SO ₃ ⁻	182.7

Figure 4.1. Ratio of $F(CF_2)_nSO_3^-/DS^-$ signal intensities in mass spectra of aqueous $[F(CF_2)_nSO_3^- + 0.2 \mu M \text{ dodecyl sulfate}]$ solutions at pH 6.0 as functions of F -surfactant concentration. Lines are linear regressions to the experimental data ($R^2 > 0.99$). Linear plots were also obtained for $F(CF_2)_nCO_2^-$. Error bars contained within symbol size.

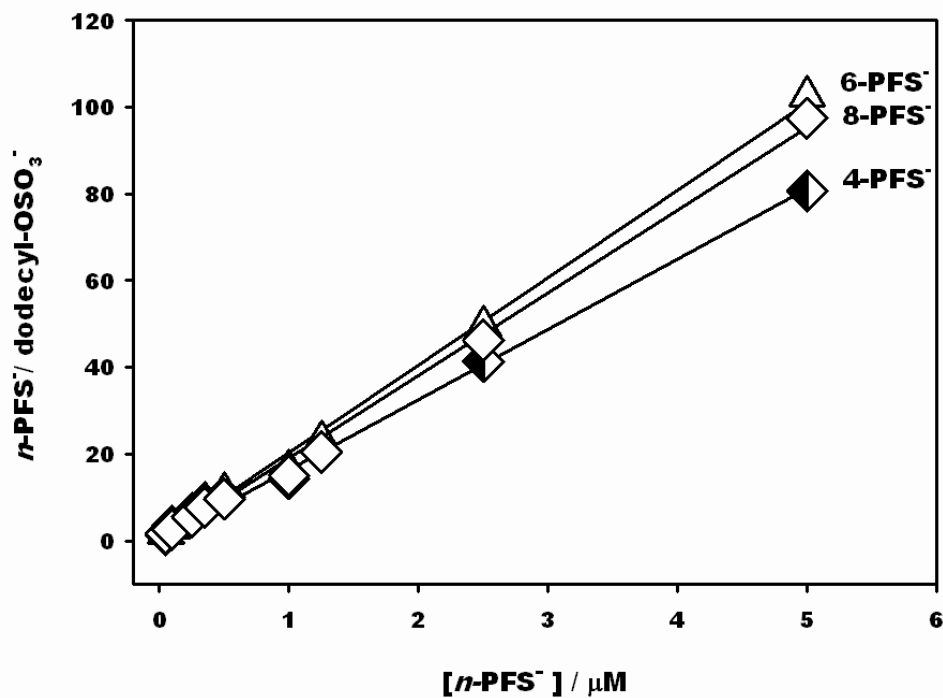


Figure 4.2 Electrospray ionization mass spectrum of a 1 μM equimolar multianion aqueous solution at pH 7. Signal intensities S normalized to $(S_{79} + S_{81}) \equiv 1$ (see text for details). The inset is a semilogarithmic plot. Blue and red drop lines and legends correspond to $\text{F}(\text{CF}_2)_n\text{CO}_2^-$ and $\text{F}(\text{CF}_2)_n\text{SO}_3^-$ surfactants, respectively. DS is dodecyl sulfate.

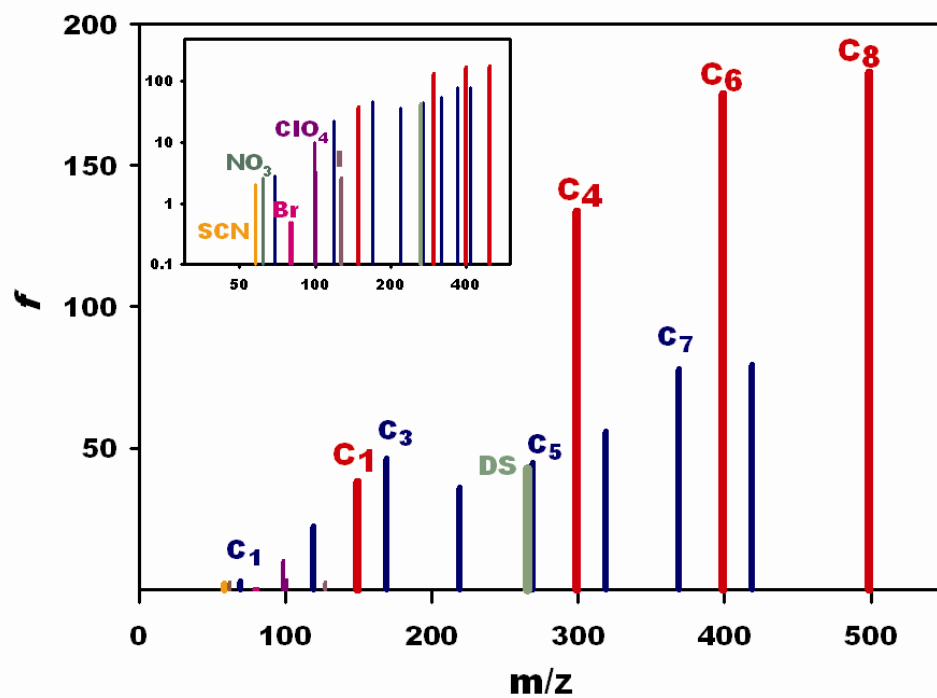


Figure 4.3. Enrichment factors f versus n -alkyl chain length. Gray-red symbols: $f[\text{F}(\text{CF}_2)_n\text{SO}_3^-]$. Gray-blue symbols (connected by straight lines; diamonds/circles stand for odd/even n -homologues): $f[\text{F}(\text{CF}_2)_n\text{CO}_2^-]$. All data obtained in $1\ \mu\text{M}$ solutions. S_{th} designates the theoretical $\log f$ vs. n slope predicted by equation (4.2) – (4.4) and data from References 67 and 68. Error bars contained within symbol size.

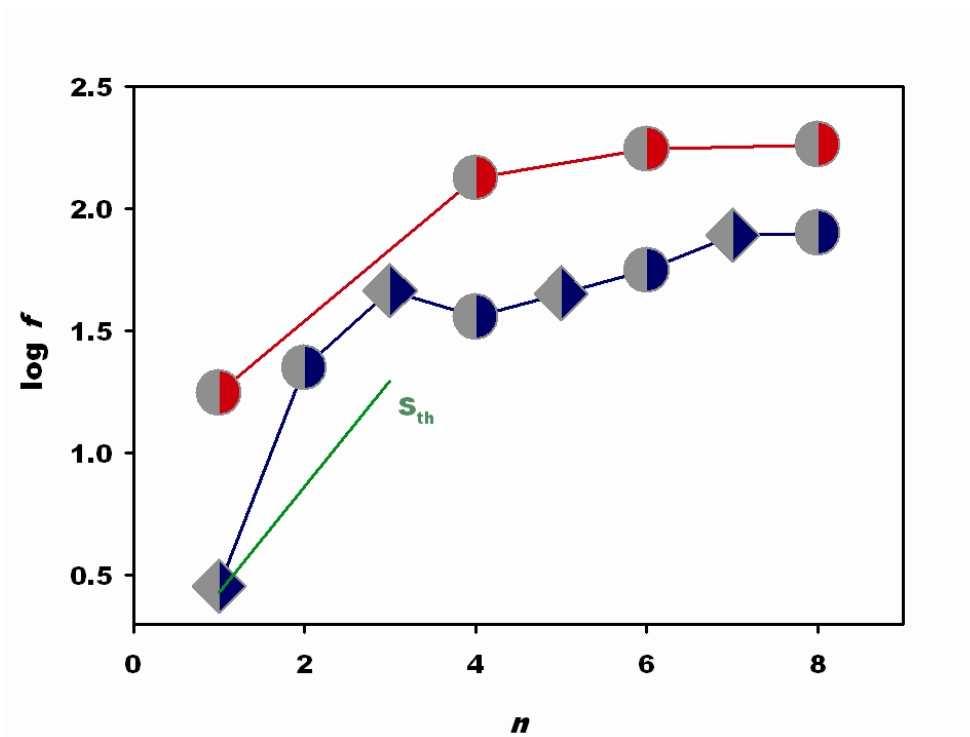
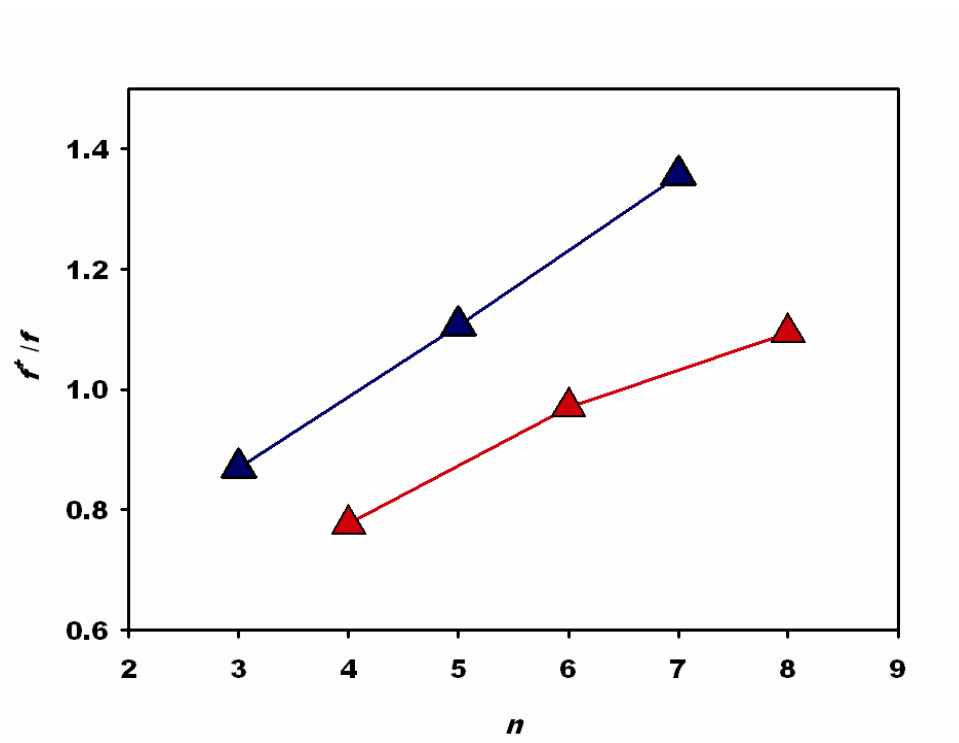


Figure 4.4. Enrichment factors ratios f^+/f for $F(\text{CF}_2)_n\text{SO}_3^-$ (red) and $F(\text{CF}_2)_n\text{CO}_2^-$ (blue) surfactants. f : in 1 μM aqueous F -surfactant solutions, f^+ : plus 100 μM NaCl and 1-octanol saturation. Error bars contained within symbol size.



Scheme 4.1. *Anti*-perfluorobutanoate (left) and *gauche*-perfluorobutanoate (right) at the air/water interface. A closer approach of fluorine atoms to the water surface minimizes the free energy of the system.^{48,64,67}

